HIGHLIGHTS

- Soil macroaggregates (4-1 and 1-0.25 mm) thin sections have been investigated

- Optical microscopy and SEM-EDS allowed the *in situ* analysis of OM in macroggregates

- Both physical occlusion and mineral interactions stabilized OM in macroaggregates

- The highest OM stabilization by both mechanisms was in fine macroaggregates

- In fine macroaggregate, both OM accumulation and functionality maintenance occurred

1   **Title**

2   **New insights into organic carbon stabilization in soil macroaggregates: an *in situ* study by optical**

3   **microscopy and SEM-EDS technique**

4

5   Authors

6   Guidi Patrizia (1), Falsone Gloria (1), Wilson Clare (2), Cavani Luciano (1), Ciavatta Claudio (1), Marzadori

7   Claudio (1)

8

9   Author Affiliations

10   (1) Dipartimento di Scienze e Tecnologie Agro-alimentari, Alma Mater Studiorum Università di Bologna,

11   40127 Bologna (I)

12   (2) Biological and Environmental Science, University of Stirling, FK9 4LA Stirling (UK)

13

14   Corresponding author

15   Gloria Falsone, email gloria.falsone@unibo.it

16

ABSTRACT

The purpose of this study was to investigate the *in situ* characterization of organic matter (OM) within soil macroaggregates, and to assess the relationships between OM characteristics and macroaggregate size indicating different OM stabilization mechanisms. Optical micro-morphological investigations, coupled to SEM-EDS (scanning electron microscopy and energy X-ray spectroscopy) technique, were carried out on thin sections of 1-4 and 0.25-1 mm soil aggregates (coarse and fine macroaggregates, respectively) from 0-20 cm soil layer corresponding to A horizon of four different sites in which soil structure were not disturbed by tillage.

The intraggregate porosity, measured by image analysis of four different size classes (<50, 50–100, 100–200, >200 µm), showed that fine macroaggregates were significantly less porous (3.70-6.71% of total porosity) and had higher presence of the finest pore class (<50 µm) compared to coarse macroaggregates (5.93-9.08% of total porosity), independently from sites. The percentage of organic matter forms (OMFs) identified by optical investigation was significant higher in fine (13.5-17.7%) than in coarse (4.19-8.27%) macroaggregates. In particular, fine macroaggregates were richer in red and black amorphous organic forms, which were characterized by the highest values of Al:C, Fe:C and Ca:C molar ratios. These findings suggested thus an accumulation of OM in fine macroaggregates than in coarse macroaggregates occurred. It was probably due to a more efficient OM stabilization in fine than in coarse macroggregates related to both physical occlusion (lower porosity and smaller pore size) and organo-minerals interaction (higher presence of OMFs characterized by the highest Al:C, Fe:C and Ca:C ratios),

The OM exposure index (EI), a measurement of the OM surface exposed to pores and thus potentially available for microbial activity, was unexpectedly higher in fine than in coarse macroaggregates (EI: 0.48-0.79 and 0.25-0.58 mm^{-1} in fine and coarse macroaggregates, respectively). However, the accessibility of OM defined by the EI seemed to facilitate neither the oxidative transformation nor the damage of enzyme activities, being the EI positively related to C:N ratio (r=0.66), negatively to δ^{13}C values (r=-0.74) and positive to the geometric mean of the five assayed enzyme activities related to C-cycle (r=0.79). Therefore, even more potentially exposed, in fine macroaggregates the OM was not accessible to microorganisms due to the

43   effective physical occlusion, and thus both accumulation of few transformed OM and maintenance of

44   functionality related to C-cycle occurred.

45   The OM stabilization in macroaggregates thus involved both physical occlusion and organo-metals/mineral

46   phase interactions processes. Both these processes are often related to microaggregates rather than

47   macroaggregates. Our findings thus seem to provide a new insight for studying the potentiality of OM

48   stabilization and C sequestration in soil macroaggregates.

49

50 **KEYWORDS**

51 Macroaggregate size; aggregate thin sections; optical microscopy; SEM-EDS; physical occlusion; organo-

52 mineral interactions.

53

1. INTRODUCTION

The largest amount of organic C in terrestrial ecosystems is in the soil and it is three time the amount of C in the atmosphere and four time that in the biota (Janzen, 2004). The persistence of this high amount of organic matter (OM) in soil depends on many factors including land use, edaphic factors and climate (Smith et al., 2008), and can be altered by human activities, which can indeed have contrasting effects (Bai et al., 2018; Baude et al., 2019; Lal, 2004a; Lal, 2004b; Lal et al., 2015). One of the objectives of the current soil science research is to model, in a reliable way, the flow of C from, within, and to the soil in order to allow the assessment of the different soil properties and management practices applied. To date, one of the main difficulties in reaching this goal is given by the lack of sufficiently detailed knowledge on the processes that govern the persistence of the soil OM (Schmidt et al., 2011).

Several authors consider that, for a mechanistic understanding and modelling of soil OM decomposition and stabilization, it is crucial to improve knowledge on processes such as occlusion of organic matter within aggregates and sorption of organics onto mineral surfaces (Kögel-Knabner et al., 2008). Conant et al. (2011) proposed a conceptual model defining the resistance of soil OM to decomposition as being due to its chemical structure and its physicochemical protection. The former referred to the de-polymerization process, the latter to adsorption/desorption on mineral surface and aggregate turnover. Recently, Wiesmeier et al. (2019) stressed the role of physical protection within aggregates for soil OM persistence, stating that physical protection, and therefore the aggregation process itself, must be considered as an important mechanism for stabilization of organic C.

The physical protective capacity of aggregates to soil OM is related to the spatial separation of substrate and microorganisms, as well as to reduced microbial activity due to a lower diffusion of gasses into and within aggregates (Mikutta et al., 2006; Six et al., 2002). Kravchenko et al. (2015), combining CO_2 respiration measurements with X-ray computed micro-tomography imaging, demonstrated a feed-forward relationship between particulate organic matter decomposition and pore connections in intact soil samples. Furthermore, organo-mineral associations acting in soil OM protection can be considered as structural units of soil

5

79 aggregates and nanoparticulate fractions of the smaller aggregates themselves (Totsche et al., 2017), and

80 are, therefore, strictly related to the aggregate formation process.

81 Six et al. (2000) postulated that SOM stabilization is based on microaggregate (<0.25 mm) formation within

82 macroaggregates (>0.25 mm), with C in microaggregates stabilized and sequestered for the long-term.

83 Macroaggregates would instead provide minimal C physical occlusion (Six et al., 2004). The efficiency of

84 macro- and microaggregates in soil OM stabilization is due to the different mechanisms that generate

85 aggregates of different size, as extensively described (e.g., Six et al., 2004). However, the role of

86 macroaggregates is essential in soil OM stabilization; macroaggregates being important environment where

87 both organic C is preferentially accumulated and microaggregate formation occurs (Gioacchini et al., 2016;

88 Six et al., 2000).

89 In addition to the aggregate size, the extent of the C transformation and stabilization in aggregates can be

90 influenced by the network of the intraggregate pores (Toosi et al., 2017), and by the OM exposure to the

91 pore surface (Ananyeva et al., 2013). The exposure of the OM to the pores surface can influence the contact

92 with the gaseous and biotic phase of the soil, two fundamental factors in the transformation OM processes.

93 We suggest thus that the localization of the OM within the aggregates is an aspect that needs to be taken

94 into account and demands in-depth investigation.

95 Optical micro-morphological investigations of soil aggregate thin sections allows researchers to localize soil

96 OM in an undisturbed physical space within aggregates and, coupling them with SEM-EDS analysis, to

97 investigate *in situ* characteristics of OM. Considering that C preferentially accumulates in macroaggregates,

98 and that the processes leading to the long-term soil OM stabilization begins within macroaggregates (i.e., the

99 microaggregates formation begins within macroaggregates), we believe that a study of OM properties within

100 macroaggregates can provide new insights into the understanding of the processes of organic carbon

101 preservation into soil aggregates.

102 For this, optical micro-morphological investigations, coupled SEM-EDS technique, of thin sections of

103 macroaggregates of different size (1-4 mm coarse macroaggregates, 0.25-1 mm fine macroaggregates) were

104 carried out to study *in situ* OM properties. In order to increase our knowledge on soil OM persistence, the

current research examined these microfeatures in soils characterized by different site conditions in two mountain and plain areas in the Northern Italy.

Specifically, this study focused on (i) the *in situ* characterization of soil organic matter within coarse and fine macroaggregates from soil in different site conditions, and (ii) the existence of relation between OM characteristics and macroaggregate size suggesting specific OM stabilization processes. We investigated four soils from sites that differed in key drivers of OM persistence, such as climate, soil properties and management (Wiesmeier et al., 2019) because we would test if the hypothesized relationships between OM characteristics and macroaggregate size were similar among different sites (i.e., sites which differed in climate, soil properties and management) and thus if a certain size-effect exists transgressing the environmental key properties.

2. MATERIALS AND METHODS

2.1. The study area

In this study we investigated both mountain and plain areas of different altitudes in the Emilia Romagna region (Northern Italy). The mountain area was located at Monzuno in the Appennine mountain, while the plain area was at Cadriano in the Po Valley (Table 1). The soils in the mountain area formed on limestone-marl and pelitic-sandstone stratifications, while those in the plain area develop on conoids, i.e. sedimentary bodies consisting of a clastic sediment accumulation. Both soils are ascribed to Inceptisols (Soil Survey Staff, 2014) as evinced from the Regional Soil Survey Service database (Regione Emilia Romagna, 2018). The climate of the mountain area is characterized by mean annual temperature of 11.6°C and mean annual precipitation of 967 mm, while in plain area by 12.9°C and 645 mm, respectively.

In both areas we selected two sites on the basis of soil management (Table 1), avoiding agricultural sites subject to annual tillage operations that would strongly affect soil aggregation (Bronick and Lal, 2005). In the mountain area, we thus selected a 16-yrs old oak wood (M-OW) and a 5-yrs old alfalfa (M-AA.). In the plain area we investigated an experimental walnut grove of the cv. Lara in place since 2001 selecting one fertilized area (P-FF) receiving 90 kg urea ha^{-1} y^{-1} as granular urea and one non-fertilized control area without urea

131 distribution (P-NF). In each site, two different plots have been selected and pits wide about 0.3 m were dug.

132 From each pit, the 0-20 cm soil layer corresponding to A horizon was collected. The main physico-chemical

133 properties of the fine earth of 0-20 cm topsoil were reported in Table 1S.

134 All soil samples were air dried at room temperature and sieved in order to obtain the macroaggregate

135 fraction (>0.25 mm; Six et al. 2000; Tisdall and Oades, 1982). The macroaggregates have been further divided

136 by dry-sieving into coarse macroaggregates (1-4 mm) and fine macroaggregates (0.25-1 mm) using a 1 mm

137 sieve in agreement with experimental evidence (e.g., Legout et al., 2005; Lu et al., 2016) indicating that

138 aggregates >1 mm might have lower stability, and thus higher turnover, than aggregates <1 mm.

139

140 *2.2. Soil aggregate thin sections preparation*

141 The aggregates in both macroaggregate classes have been gently mixed and at least 25 and 50 aggregates

142 have been randomly kept for the preparation of thin section of the coarse and fine macroaggregate,

143 respectively. Water was removed from the aggregates by air-drying to avoid C losses during the acetone

144 replacement drying process. No accommodating crack voids were identified in the air-dried thin sections,

145 suggesting that shrinkage and cracking during the drying process had been minimal. The method for

146 preparing thin section was based on Takeda (1988) and Tippkötter et al. (1986). Blocks of aggregates were

147 obtained by impregnation of aggregates samples with polyester resin. The blocks have been then cut along

148 a diameter plane, shaven out and glued to the slide. The slices were thinned to a standard thickness of 30-

149 40 μm, using the Logitech precision lapping machine. The slices were further reduced to few μm and hand-

150 polished by rubbing the slices on paper coated using the birefringence colours of the minerals as indicated in

151 the Michel-Levy paper which reports the birefringence colours of individual minerals according to their

152 thickness. Finally, aggregates thin sections (28 x 48 mm) were polished using diamond paste. The slides were

153 not cover-slipped since the organic microfeatures in these thin-sections were to be analysed for their

154 elemental composition by scanning electron microscope (SEM) equipped with an EDS probe.

155

156 *2.3. Optical micromorphology observations, image analysis of pores and organic components in the*

157 *aggregate thin sections*

158 Conventional descriptions of thin sections were made at 40X following the guidelines of Stoops (2003) and

159 Fitzpatrick (1980). To achieve our research aim, the area of interest in each thin section in this study

160 corresponded to the intraggregate area. Measurements on aggregates close to the edge of the thin sections

161 or having inside/near artificial bubbles were avoided, and consequently in coarse macroaggregate thin

162 sections from 9 to 16 single aggregates were analysed for each site, while in fine macroaggregate thin

163 sections from 23 to 41 aggregates were investigated. Optical observations have been carried out using a

164 polorised microscope Olimpus BX50.

165 For image analysis of intra-aggregates porosity and organic matter, high-resolution images were captured at

166 40x using a digital camera, and connected to a computer equipped with an images frame grabber. Captured

167 images were then available for computerised analysis carried out by AnalySIS v 510 (Olympus Soft Imaging

168 Solutions GmbH) image analysis software. Image analysis provides quantitative information from the

169 scanned image.

170

171 *2.3.1. Total porosity and pore size distribution*

172 To measure pores, multiple images of the same representative aggregates were taken under both plane (PPL;

173 Figure S1-a) and crossed polarized light (XPL) at 0.5 and 15° (Falsone et al., 2014). This was necessary to

174 distinguish between pores and quartz, since both were translucent under PPL. These images were additively

175 combined and the result inverted. The inverted images were multiplicatively layered with a natural light

176 image to produce a composite binary image in which minerals were readily distinguished from voids, with

177 minerals and soil matrix represented by black pixels and pores by white pixels (Figure S1-b; Hallaire et al.,

178 2000; Nakatsuka and Tamura, 2016). To exclude any electronic noise and difficulties in removing quartz, the

179 minimum size for detecting pores was set at 100 μm^2.

180 The pores were classified according to four different size classes (Pagliai et al,. 2004; Zhou et al., 2012): <50,

181 50–100, 100–200, >200 μm, on the basis of their equivalent diameters. The total surface of pores and the

182   surface of each pore classes were measured. The percentage of total porosity (total porosity %, i.e., total

183   surface of pores/surface of investigated area) and pore size distribution (% of <50, 50–100, 100–200, >200

184   µm; i.e., surface of each pore class/total surface of pores) were thus calculated.

185

186   *2.3.2.   Total surface of organic matter forms (OMFs) and their distribution*

187   Under PPL and XPL conditions, the organic forms were identified and categorized as being either organ or

188   amorphous in form (Babel, 1975; Figure S2). Once classified according to their form, organic components

189   have been further described according to the extent of their decomposition following the classification

190   proposed by Fitzpatrick (1993) where amorphous forms were strongly decomposed organic fragments, and

191   were further described by their colour, with change in colour from yellow to red and black indicating greater

192   decomposition due to oxidative and microbial processes (Bullock et al., 1985; Figure 2). A manual delimitation

193   of each organic component has been provided using image analysis software within PPL images (Figure S1-

194   c). Images were thus segmented selecting for organic fragments, and the total area of organic fragments and

195   the area of each class of organic features was measured.

196   The percentage of total surface of organic forms (organic matter forms %, i.e., surface of organic forms/

197   surface of investigated area) was calculated. The distribution of different organic components recognised (%

198   of organs and amorphous forms, classified according to their decomposition degree and colour, respectively)

199   was also calculated (i.e., surface of each organic form/surface of investigated area).

200

201   *2.3.3.   Organic matter-pores contact: the exposure index (EI)*

202   The images obtained by organic components analysis was exported and stacked upon the binary pore image

203   thereby forming a map showing the distribution of organic matter in relation to soil pores. It was thus possible

204   to identify the surface of organic matter in contact to the pores and to measure the length of contact

205   perimeter between the two features. Then, the total length of the contact perimeter (in mm) was normalized

206   by the total area of organic form (in mm^2), in order to obtain a measure of the proportion of the organic

207   matter surface in contact to the pore. For each sample, an index, called exposure index (EI; mm^{-1}) was

208   calculated. The EI gives information about the organic matter-pores contact, and therefore on the potential

209   physical exposure of organic matter to the microbial activity (Young et al., 2008).

210

211   *2.4. SEM-EDS analysis on the aggregate thin sections*

212   Polished thin sections were analysed using an environmental scanning electron microscope (SEM) and

213   elemental data were collected by energy-dispersive spectroscopy (EDS) detector using ZEISS SEM systems

214   (EVO MA15) linked to an Oxford Instruments INCA X-max detector with an 80-mm^2 SDD. For this work, the

215   instrument setup was: low vacuum conditions (>30 kPa), accelerating voltage of 5-20 keV, process time of

216   5.0, working distance of 8.5 mm, spot-size between 500-560. EDS analysis was performed at high

217   magnifications (500-1000x). The microanalysis was carried out for the detected organic features (Figure S2)

218   in coarse and fine macroaggregates. About 50 points were scored for each organic feature. Data was

219   normalized to 100%, giving a semi-quantitative measure of elemental concentrations. Thus elemental molar

220   ratios are discussed in this work rather than absolute concentrations. Additionally, using elemental molar

221   ratios any C resin effect has been avoided. The ratios are thus being interpreted relative to one another rather

222   than being presented as actual soil ratios.

223   In this work we took into account the Al:C, Fe:C and Ca:C molar ratios as indicators of the degree of organic-

224   metals/minerals interactions (Falsone et al., 2014).

225

226   *2.5. Aggregate properties measured on aggregate fractions separated by sieving*

227   In order to check the relationships between the features measured *in situ* on aggregate thin sections and

228   chemical and biochemical aggregate properties, the organic carbon, total nitrogen, δ^{13}C signature and

229   enzyme activities related to carbon cycle have been measured on each macroaggregate class obtained by

230   dry-sieving.

231

232   *2.5.1. Organic C, total N and δ^{13}C*

For each aggregate fraction separated by dry-sieving, a representative subsample has been kept and finely ground (<0.5 mm). The total organic C (g C $kg^{-1}_{aggregate}$) and total N (g N $kg^{-1}_{aggregate}$) concentration were determined on about 10-15 mg of finely ground aggregate subsamples by dry combustion (CHNS-O Elemental Analyser 1110, Thermo Scientific GmbH, Dreieich, DE). The relative abundance of C stable isotopes was determined by continuous flow- isotope ratio mass spectrometry (CF-IRMS) using an isotopic mass spectrometer Delta V advantage (Thermo- Finnigam, DE). The values were then expressed as δ^{13}C, as deviation in parts per thousand compared to the universal reference standard.

2.5.2. The geometric mean of enzyme activities (GMea)

For each aggregate fraction separated by dry-sieving, enzyme activities have been measured using about 2 g of samples. The geometric mean of the assayed enzyme activities (GMea) was used as a comprehensive index of soil quality in order to compare enzyme activities in coarse and fine aggregates (Liu et al., 2013). For each aggregates class the geometric mean of the assayed enzyme activities (GMea) was calculated as:

$$GMea = \sqrt[5]{\beta - GLU \cdot \alpha - GLU \cdot N - AG \cdot \beta - XYL \cdot \beta - CEL} \qquad (1)$$

where β-GLU, α-GLU, N-AG, β-XYL and β-CEL were β-glucosidase, α-glucosidase, N-acetyl β-glucosaminidase, β-xylosidase, β-cellobiosidase, respectively. These enzyme activities were chosen on their relevance for C cycle (Liu et al., 2013, Qin et al., 2010). The activity of these five extracellular hydrolytic enzymes was determined using MUF conjugates at final concentrations (Microplate fluorometer infinite200, TECAN, Männedorf, CH) ensuring substrate saturating conditions in according to Giacometti et al. (2014).

2.6. Statistical analysis

Differences in the micromorphological features (porosity, organic forms, EI) between coarse and fine macroaggregaes (size factor) were checked by the one-way ANOVA.

Differences in the molar ratio (Al:C, Fe:C and Ca:C), determined from EDS analysis, among organic forms and between coarse and fine macroaggregates in thin section were tested by the one-way ANOVA.

259 The assumption of ANOVA was tested by Shapiro-Wilks test for normality and data distribution and Levene

260 test for homogeneity of variances.

261 The relationships between EI micromorphological property and both the chemical and biochemical

262 properties measured on the aggregates were evaluated using the Pearson's correlation coefficient.

263 The threshold used for significance in all statistical tests was set at 0.05. All data treatments were carried out

264 using R *agricolae* package (R core team, 2019).

265

266 **3. RESULTS**

267 *3.1. Porosity*

268 The total detectable porosity, measured in the intraggregates space, ranged from 5.93 to 9.08% and from

269 3.70 to 6.71% in coarse and fine macroaggregates, respectively (Table 2). Porosity varied significantly based

270 on size factor ($p < 0.001$), and the fine macroaggregates were less porous than the coarse ones (Table 2).

271 Within each aggregate class, among sites no differences in the intraggregate porosity were found.

272 Figure 1 (a-b) shows the pore size distribution (PSD) in the different aggregates. The PSD was significantly

273 influenced by the size factor ($p < 0.01$; Figure 1-c). The pores >200 μm were only present in coarse

274 macroaggregates, while in fine macroaggregates pore <50 μm predominated. Fine macroaggregates,

275 therefore, were significantly less porous and showing finer porosity compared to coarse macroaggregates.

276 Between sites, no differences in the PSD were found (Figure 1-c).

277

278 *3.2. Organic C concentration and organic matter forms (OMFs)*

279 The concentration of organic C in aggregates, measured on ground samples, varied from 6.6 and 49.6 g kg^{-1}

280 and from 7.8 and 52.4 g kg^{-1} in coarse and fine macroaggregates, respectively (Table 2). The organic C content

281 of fine and coarse macroaggregates was therefore characterized by a high variability, but it was possible to

282 observe a tendency for which the accumulation of C significantly increased passing from the coarse to the

283 fine macroaggregates within each site (p always <0.01; Table 2). The percentage of OMFs, measured on

284 aggregate thin sections, varied from 4.19 to 8.27 and from 13.54 to 17.75% in coarse and fine

285 macroaggregates, respectively (Table 2), confirming that accumulation of organic matter was higher in fine

286 than in coarse macroagrregates (p<0.001). The percentage of OMFs on macroaggregates thin section and

287 organic C concentration measured by dry combustion on ground aggregates showed thus a significant similar

288 trend (r=0.567, p<0.05).

289

290 *3.3. OMFs distribution and Al:C, Fe:C and Ca:C molar ratios*

291 The OMFs detected on thin sections were differently distributed between aggregates (Table 3): the organs

292 have been detected only in coarse macroaggregates of mountain sites, while the organic amorphous forms

293 have been found both in coarse and fine macro-aggregates. The lack of organs in the plain area evidenced

294 difference according sites, which was confirmed also for amorphous forms (p<0.05). However, independently

295 from the sites, according to the size factor the fine macroaggregates were clearly the richest in red and black

296 organic amorphous forms (p<0.001).

297 Coupling the optical analysis to the SEM-EDS technique, it was possible to perform a semi-quantitative

298 measurement of the element concentrations for each identified OMFs class. In particular, Al:C, Fe:C and Ca:C

299 molar ratios of each OMFs class in coarse and fine macro-aggregates were determined (Figure 2). The

300 morphologically recognised OMFs showed different values of molar ratios. In particular, red and black

301 amorphous forms were characterized by the highest values of Al:C and Fe:C (p<0.05) and black amorphous

302 forms had also the highest values of Ca:C molar ratios (p<0.05). This occurred both in coarse and fine

303 macroaggregates.

304 *3.4. Exposure Index (EI)*

305 The EI values (Figure 3) varied from 0.25 to 0.58 mm^{-1} in coarse macroaggregates and from 0.48 to 0.79 mm^{-}

306 ^{1} in fine macroaggregates, being significantly higher in fine macroaggregates (p<0.05). Figure 4 showed the

307 relationships between EI values and both C/N ratio and δ^{13}C values. Specifically, EI values was positively

14

308 correlated to the C/N ratio and negatively to the δ^{13}C values. The EI was significantly positively correlated

309 also to GM*ea* (Figure 5).

310

311 **4. DISCUSSION**

312 *4.1 The effect of macroaggregate size on OM characteristics*

313 One of the objectives of our work was to characterize soil organic matter (OM) fractions according to their

314 specific physical location within the fine and coarse macroaggregates (*in situ*). Technically this was performed

315 through optical investigation of aggregate thin sections which allowed us the *in situ* identification and

316 quantification of organic matter forms (OMFs). The quantification of OM was also performed on ground

317 samples by the well-standardized dry combustion method, which provides the quantification of the whole

318 organic C in disturbed samples without any distinction among different forms. The quantification of OM

319 content in the aggregates obtained by the two methods (i.e., the content of OC in ground aggregates and the

320 presence of OMFs detected on aggregate thin section) showed similar trend and the data was significantly

321 related.

322 The *in situ* quantification of OMFs showed that fine macroaggregates were richer in organic matter than

323 coarse ones. Organic C accumulation in small aggregates is often reported (Six et al., 2000; Six et al., 2004;

324 Tisdall and Oades, 1982), and in general this C-enrichment refers to microaggregates (i.e, aggregate <0.25

325 mm). Our findings thus showed that C accumulation can occur also in small macroaggregates of 0.25-1 mm

326 size class. Additionally, our data showed that OC accumulation in fine macroaggregates was coupled to a

327 decrease in porosity. In fact, the effect of macroaggregate size was also observed in the aggregate porosity,

328 with the lowest porosity and the smallest pore size in the fine macroaggregate class. In our opinion, thus, the

329 lowest porosity and smallest pore size in fine macroaggregates could enhance the persistence of OM. The

330 effect of pores network on soil OM stabilization has been in fact observed by several authors. Toosi et al.

331 (2017) demonstrated by their long-term experiment that, in natural succession system, the abundance of

332 specific size classes of pores affected OM decomposition and thus its chemistry in macroaggregates.

333 Kravchenko and Guber (2017) reported experimental evidences indicating pores of 30-90 μm in size as drivers

15

334 in processes of organic carbon decomposition. Ananyeva et al. (2013) showed that abundance of 40-70 µm

335 pores was negatively correlated with levels of organic carbon in macroaggregates, suggesting that aggregates

336 with great amount of such pores poorly protected organic matter. Quigley et al. (2018) agreed that pores of

337 40–90 µm size range are associated with quick organic C decomposition, while pores <40 µm tend to be

338 associated with C protection. Yang et al. (2019) suggest that total porosity has a significant role, increasing

339 soil aggregate organic carbon respiration. With regard to our data, we suggest that the highest total porosity

340 could have favored a greater degradation of organic matter in coarse macroaggregates, and that conversely

341 the greatest percentage of pores <50 µm in fine macroaggregates, according to cited authors, could have

342 contributed to organic matter storage within them. Therefore, in our study the physical occlusion would be

343 more efficient in fine macroaggregates than in coarse ones.

344 The effect of size classes of macroaggregates on physical occlusion seemed to transgress that of the site

345 conditions, being both porosity and OMFs amount similar within fine and coarse macroaggregates. This

346 finding was quite unexpected, because site conditions (climate, parent material, soil texture, soil OM, etc.)

347 are considered as key factors in the aggregation process (e.g., Bronick and Lal, 2005; Saker et al., 2018).

348 However, in our study a certain site effect has been detected on organic C content of ground aggregates.

349 Thus, even if clearly the aggregate size strongly affected the physical occlusion of OM, we can not completely

350 excluded a specific site effect on OM stabilization. The OMFs distribution in fact differed among sites: in the

351 aggregates from the soils located in the plain areas organs completely lacked while they were present in the

352 coarse macroaggregates of soils in the mountain areas. Fitzpatrick (1993) and Ismail-Meyer et al. (2018)

353 suggested that organs consist of plant residues containing cells and represent thus less transformed soil OM.

354 The presence of less transformed soil OM in mountain areas was indeed in agreement with the well-known

355 slowing down of organic matter oxidative kinetics due to low temperature (e.g., Cardelli et al., 2019; De

356 Feudis et al., 2019) allowing at higher altitude greater accumulation of less transformed OM in mountain soils

357 than in plain ones. No general trend has been instead detected in amorphous forms, that according to

358 Fitzpatrick (1993) and Falsone at al. (2014) are the end-product of organic residues transformation.

359   Independently from sites, other processes than physical occlusion might however contribute to the higher

360   accumulation of organic matter in fine than in coarse macroaggregates. Processes related to interaction of

361   OM with minerals/metals can in fact contribute to OM stabilization (Conant et al., 2011).

362   Our data showed that OM accumulation in fine macroaggregates was due to the organic amorphous forms,

363   being organs missing in fine macroaggregates. Additionally, SEM-EDS microanalysis showed that that red and

364   black amorphous forms had the highest Al:C, Fe:C and Ca:C molar ratios. These molar ratios are chemical

365   indicators of OM stabilization reflecting the interaction of OMFs with the soil mineral phase, and high molar

366   ratio values indicate stronger organo-mineral interactions (Brown et al., 2000). OM stabilization by mineral

367   interactions was thus mainly attributable to red and black OMFs. This was in agreement with the fact that

368   red and black amorphous organic forms are the end-product of organic residues transformation (Fitzpatrick,

369   1993), and that plant residues or particulate organic matter during decomposition become encrusted with

370   mineral particles and microbial by-products in macroaggregates (Six et al., 2004). It is well-known that these

371   interactions form the core of smaller aggregates within the larger ones, increasing soil OM stabilization in

372   microaggregates (Six et al., 2004). Our data allowed to detect that OM stabilization by mineral interactions

373   was not exclusive only of microaggregates, but efficiently occurred in fine macroaggregates.

374   Finally, the increasing of OM in fine macroaggregates should be ascribe to a more efficient OM stabilization

375   by both physical occlusion and organo-mineral interactions than in coarse macroaggregates.

376

377   *4.2 The dynamics of macroaggregates and organic matter stabilization*

378   The stabilization of organic matter in soil aggregate limits the oxidative processes, which generally drive the

379   transformation of soil OM. They may be in turn influenced by the degree of exposure of the OM to pores

380   interfacing with the gaseous and biotic phase (Geisseler et al., 2011). For this reason, an exposure index (EI)

381   of OM was calculated from the aggregate thin sections, and the relationships between EI and both C/N and

382    $\delta^{13}C$ values have been investigated. We interpreted the EI as an index of the potential physical exposure of

383   organic matter to microbial activity (Young et al., 2008), while the C/N ratio and the $\delta^{13}C$ signature provide

384   information the degree of transformation of organic matter. The C/N ratio is in fact an indicator of the whole

17

385   organic matter pool turnover (Bronick and Lal, 2005), and a high value of C/N suggests the presence of OM

386   with low transformed status. Isotopic carbon fractionation instead occurs during the process of organic

387   decomposition, leading to enrichment in ^{13}C due to oxidation of ^{12}C by microorganisms (Feng, 2002).

388   Consequently, lower values of δ^{13}C (more negative) correspond to less oxidized organic matter (Angers et al.,

389   1997). In our study, the C/N ratio and the δ^{13}C signature of fine and coarse macroaggregates were

390   significantly correlated (r=-0.675, p<0.01; Figure S3), confirming the data convergence related to the degree

391   of OM transformation.

392   Our findings showed that high values of EI was associated to fine macroggregates. This was quite unexpected,

393   because our data suggested higher physical occlusion of OM in fine macroaggregates due to lower porosity

394   and smaller pore size than in coarse macroaggregate. Because of the methodological procedure used for EI

395   determination, the EI measures the proximity of OM to the pore surface and thus assesses if the OM is

396   encapsulated in the soil matrix or exposed. The apparent discrepancy between great degree of OM exposure

397   and high physical occlusion in fine macroaggregates, in our opinion should be explain through the origin of

398   fine macroaggregate themselves. Organic residues must initially be accessible (i.e., exposed) to

399   microorganisms in order to form fine macroaggregates in coarse ones, in agreement with Six et al. (2004)

400   who described how the transformations of the OM represent the driving processes for the formation of fine

401   aggregates into coarse ones. Our hypothesis was thus that at least a part of the OM in fine macroaggregates

402   inherited its localisation from its initial accessibility in coarse macroaggregates, and that *i)* its initial

403   degradation allows the formation of fine macroaggregates causing OM encapsulation and *ii)* consequently

404   favouring OM stabilization. This seemed to be supported by positive correlation between EI and C/N ratio,

405   and the negative ones between EI and δ^{13}C. They in fact indicated that high values of EI, typically associated

406   with fine macroaggregates, was related to OM form with lower degree of transformation. Additionally, EI

407   was positively linked to GMea. Thus, the apparent accessibility of OM defined by the EI did not compromise

408   the C-cycle functionally related to enzyme activities related to C-cycle and thus the soil functionality was

409   preserved (Wang et al., 2015; Wang et al., 2017).

410

5. CONCLUSIONS

This study offers a picture of the processes that are active within macroaggregates (1-4 and 0.25-1 mm) and which influence the transformation and stabilization of the OM as a function of its physical location. Our *in situ* investigation has allowed us to detect that:

- Coarse macroaggregates (1-4 mm) tended to be more porous and contained lower percentages of OMFs and organic C than and fine macroaggregates (0.25-1 mm).

- Fine macroaggregates accumulated OMFs characterized by a greater interaction with the mineral soil fraction, greater degree of exposure to the pores surface, lower degree of chemical transformation and higher maintenance of C-cycle functionality than in coarse macroaggregates.

- The fractions of the OM that have undergone the greatest chemical transformations (evaluated by C/N value and $\delta^{13}C$ signature) were in coarse macroaggregates and were not those that were more stable within the aggregates of the soil, in agreement with Schmidt et al. (2011).

The data of porosity, distribution of pores and organic forms determined by image analysis, confirmed that coarse and fine macroaggregates differed, and they were physically differentiated microhabitats for microorganisms. Specifically, fine macroaggregates had organic matter closer to the pores surface than in coarse macroaggregates probably due to the origin of fine macroaggregates themselves, whose genesis begins because of the decomposition of accessible particulate organic residues within coarse macroaggregates (Figure 6). In fine macroaggregates, the interaction between OM and metals and/or mineral phase and the physical occlusion of OM lead to its stabilisation (Figure 6).

Physical occlusion and interaction with minerals thus appeared as two complementary mechanisms enhancing OM stabilization in fine macroaggregates. Both these processes are often related to microaggregates (<0.25 mm) rather than macroaggregates (>0.25 mm) and further researches need on the study of their relative importance in fine macroaggregates. For example, the application of other techniques able to study intact (i.e, non-destroyed) aggregates and the three-dimensional nature of OM and pores distribution, might provide useful information on the physical protection of OM within soil

aggregates. However, our findings seem to provide a new insight for studying the potentiality of OM stabilization and C sequestration in soil macroaggregates.

REFERENCES

Angers, D., Chenu, C., 1997. Dynamics of soil aggregation and C sequestration, in: Lal, R., Kimble, J.M., Follet, R.F., Stewart, B.A. (Eds.), Soil processes and the carbon cycle. Advances in Soil Sciences (col.), Boca Raton, CRC Press, pp. 199-223.

Ananyeva, K., Wang, W., Smucker, A.J.M., Rivers, M.L., Kravchenko A.N., 2013, Can intra-aggregate pore structures affect the aggregate's effectiveness in protecting carbon? Geoderma 287, 31-39.

Babel, U., 1975. Micromorphology of Soil Organic Matter, in: Gieseking, J.E. (Ed.), Soil Components. Springer, pp. 369-473.

Bai, Z., Caspari, T., Gonzales, M.R., Batjes, N.H., Mader, P., Bunemann, E.K., de Goede, R., Brussard, l., Xu, M., Ferreira, C.S.S., Reintam, E., Fan, H., Mihelic, R., Glavan, M., Toth, Z., 2018. Effects of agricultural management practices on soil quality: A review of long-term experiments for Europe and China. Agr. Ecosyst. Environ. 265, 1-7.

Baude, M., Meyer, B.C., Schindewolf, M., 2019. Land use change in an agricultural landscape causing degradation of soil based ecosystem services. Sci. Total Environ. 659, 1526-1536.

Bronick, C.J., Lal, R., 2005. Soil structure and management: a review. Geoderma 124: 3-22.

Brown, G.G., Barois, I., Lavelle, P., 2000. Regulation of soil organic matter dynamics and microbial activity in the drilosphere and the role of interactions with other edaphic functional domains. Eur. J. Soil Biol. 36, 177-198.

461 Bullock, P., Federoff, N., Jongerius, A., Stoops, G., Tursina, T., 1985. Handbook for soil thin section description.

462 Waine Research, Wolverhampton.

463 Cardelli, V., De Feudis, M., Fornasier, F., Massaccesi, L., Cocco, S., Agnelli, A., Weindorf, D.C., Corti, G. 2019.

464 Changes of topsoil under Fagus sylvatica along a small latitudinal-altitudinal gradient. Geoderma 344 164–

465 178.

466 Conant, R.T., Ryanu, M.G., Agren, G., Birge, H., Davidson, E.A., Eliasson, P.E., Evans, S.E., Frey, S.D., Giardina,

467 C.P., Hopkins, F.M., Hyvonen, R., Kirschbaum, M.U.F., Lavallee, J.M., Leifeld, J., Parton, W.J., Steinweg, J.M.,

468 Wallestein, M.D., Wettersted, J.A.M., Bradford, M. A., 2011. Temperature and soil organic matter

469 decomposition rates- synethesis of current knowledge and way forward. Global Change Biol. 17, 3392-3404.

470 De Feudis, M., Cardelli, V., Massaccesi, L., Trumbore, S.E., Vittori Antisari, L., Cocco, S., Corti, G., Agnelli, A.

471 2019. Small altitudinal change and rhizosphere affect the SOM light fractions but not the heavy fraction in

472 European beech forest soil. Catena 181, 104091.

473 Falsone, G., Wilson, C.A., Cloy, J.M. Graham, M.C., Bonifacio, E., 2014. Relating microfeatures of organic

474 matter to C stablisation: optical microscopy, SEM-EDS, abiotic oxidation. Biol. Fertil. Soils 50, 623-632.

475 Feng, X., 2002. A theorethical analysis of carbon isotope evolution of decomposing plant litters and soil

476 organic matter. Global Biogeochem. Cy. 16, 1119.

477 Fitzpatrick, E.A., 1980. Soils: their formation, classification and distribution. London, Longman.

478 FitzPatrick E.A., 1993. Soil microscopy and micromorphology. J Wiley & Sons, Chichester.

479 Gee, G., Bauder, J.W., 1986. Particle-size analysis, in: Klute, A. (Ed.), Methods of soil analysis: Part1, 2nd ed.

480 Agron. Monogr. No. 9 ASA and SSSA, Madison, WI, pp. 383-411.

481 Geisseler, D., Horwath, W.R., Scow, K.M., 2011. Soil moisture and plant residue addition interact in their

482 effect on extracellular enzyme activity. Pedobiologia 54, 71-78.

483 Giacometti, G., Cavani, L., Baldoni, G., Ciavatta, C., Marzadori, C., Kandeler, E., 2014. Microplate-scale

484 fluorometric soil enzyme assays as tools to assess soil quality in a long-term agricultural field experiment.

485 Appl. Soil Ecol. 75, 80–85.

486 Gioacchini, P., Cattaneo, F., Barbanti, L., Montecchio, D., Ciavatta, C., Marzadori, C., 2016. Carbon

487 sequestration and distribution in soil aggregate fractions under Miscanthus and giant reed in the

488 Mediterranean area. Soil Till. Res. 163, 235-242.

489 Hallaire, v., Curmi, P., Duboisset, A., Lavelle, P., Pashanasi, B. 2000. Soil structure changes induced by the

490 tropical earthworm *Pontoscolex corethrurus* and organic inputs in a Peruvian ultisol. Eur. J. Soil Biol. 36,

491 35–44.

492 Heckman, K., Lawrence, C.R., Harden, J.H., 2018. A sequential selective dissolution method to quantify

493 storage and stability of organic carbon associated with Al and Fe hydroxide phases. Geoderma 312, 24-35.

494 Ismail-Meyer, K., Stolt, M.H., Lindbo, D.L., 2018. Chapter 17 - Soil Organic Matter. In: Stoops, G., Marcelino,

495 V., Mees, F. (Eds). Interpretation of Micromorphological Features of Soils and Regoliths 2th Edition,

496 Elsevier, pp. 471-512.

497 Kögel-Knabner, I., Guggenberg, G., Kleber, M., Kandeler, E., Kalbitz, K., Stefan, S., Eusterhues, K., Leinweber,

498 P., 2008. Organo-mineral associations in temperate soils: integrating biology, mineralogy, and organic matter

499 chemistry. J. Plant Nutr. Soil Sc. 171, 61-82.

500 Kravchenko, A.N., Guber, A.K., 2017. Soil pores and their contributions to soil carbon processes. Geoderma.

501 287, 31-39.

502 Kravchenko, A.N., Negassa, W.C., Guber, A.K., Rivers, M.L., 2015. Protection of soil carbon within macro-

503 aggregates depends on intra-aggregate pore characteristics. Sci. Rep. 5, 16261-16261.

504 Janzen, H.H., 2004. Carbon cycling in earth systems-a soil science perspective. Agr. Ecosyst. Environ. 104,

505 399-417.

506 Lal, R., 2004a. Soil carbon sequestration impacts on global climate change and food security. Science 304,

507 1623-1626.

508 Lal, R., 2004b. Soil carbon sequestration to mitigate climate change. Geoderma 123, 1-22.

509 Lal, R., Negassa, W., Lorenz, K., 2015. Carbon sequestration in soil. J. Environ. Sustain. 15, 79-86.

510 Legout, C., Leguédoi, S., Le Bissonnais, Y., 2005. Aggregate breakdown dynamics under rainfall compared

511 with aggregate stability measurements. Eur. J. Soil Sci. 56, 225-237.

512   Liu, Y. R., Li, X., Shen, Q. R., & Xu, Y. C., 2013. Enzyme activity in water-stable soil aggregates as affected by

513   long-term application of organic manure and chemical fertiliser. Pedosphere 23, 111–119.

514   Lu, J., Zheng, F., Li, G., Bian F., An, J., 2016. The effects of raindrop impact and runoff detachment on hillslope

515   soil erosion and soil aggregate loss in the Mollisol region of Northeast China. Soil Till. Res. 161, 79-85.

516   Mikutta, R., Kleber, M., Torn, M.S., Jahn R., 2006. Stabilization of soil organic matter association with minerals

517   or chemical recalcitrance? Biogeochemistry 77, 25-56.

518   Nakatsuka, H., Tamura, K., 2016. Characterisation of soils under long-term crop cultivation without

519   fertilisers: a case study in Japan. SpringerPlus 5, 283.

520   Pagliai, M., Vignozzi, N., Pellegrini, S., 2004.Soil structure and the effect of management practices. Soil Till.

521   Res. 79, 131-143.

522   Poeplau, C., Don, A., Six, J., Kaiser, M., Benbi, D., Chenu, C., Cotrufo, M.F., Derrien, D., Gioacchini, P., Grand,

523   S., Gregorich, E., Griepentrong, M., Gunina, A., Haddix, M., Kuzyakov, Y., Kuhnel, A., Macdonald, L.M., Soong,

524   J., Trigalet, S., Vermeirc, ML., Rovira, P., van Wesemael, B., Wiesmeier, M., Yeasmin, S., Yevdokimov, I.,

525   Nieder, R., 2018. Isolating organic carbon fraction with varying turnover rates in temperate agricultural soils

526   - A comprehensive method comparison. Soil Biol. Biochem. 125, 10-26.

527   Qin, S. P., Hu, C. H., He, X. H., Dong, W. X., Cui, J. F. Wang, Y. 2010. Soil organic carbon, nutrients and relevant

528   enzyme activities in particle-size fractions under conservational versus traditional agricultural management.

529   Appl. Soil Ecol. 45: 152–159.

530   Quigley, M.Y., Negassa, W.C., Guber, A.K., Rivers, M.L., Kravchenko, A.N. 2018. Influence of pore

531   characteristics on the fate and distribution of newly added carbon. Front. Environ. Sci. 6, 51.

532   R Core Team, 2019. R: A language and environment for statistical computing.

533   Schmidt, M.W.I., Torn, M.S., Abiven, S., Dittmar, T., Guggenberger, G., Janssen, I.A., Kleber, M., Knabner, I.K.,

534   Lehmann, J., Manning, D.A., Nannipieri, P., Rasse, D.P., Weiner, S., Trumbore, S.E., 2011. Persistance of soil

535   organic matter as an ecosystem property. Research Perspective 478, 49-56.

536   Regione Emilia Romagna, 2018. Carta dei suoli della pianura, del basso e medio appennino emiliano-

537   romagnolo in scala 1:50.000. Servizio Geologico, Sismico e dei Suoli della Regione Emilia Romagna.

538 Sarker, T.C., Incerti, G., Spaccini, R., Piccolo, A., Mazzoleni, S. Bonanomi, G., 2018. Linking organic matter

539 chemistry with soil aggregate stability: Insight from 13C NMR spectroscopy. Soil Biol. Biochem. 117, 175–184.

540 Six, J., Elliot, E.T., Paustian, K., 2000. Soil macroaggregate turnover and microaggragate formation: a

541 mechanism for C sequestration under no-tillage agriculture. Soil Biol. Biochem. 32, 2099-2103.

542 Six, J., et al., 2002. Soil organic matter, biota and aggregation in temperate and tropical soils effect of no

543 tillage. Agronomie 22, 755-775.

544 Six, J., Bossuyt, H., Degryze, S., Denef, K., 2004. A history of research on the link between (micro)aggregates,

545 soil biota, and soil organic matter dynamics. Soil Till. Res. 79, 7–31.

546 Smith, P., Fang C., Dawson, J.J.C., Moncrieff. J.B., 2008. Impact of global warming on soil organic carbon. Adv.

547 Agron. 97, 1-43.

548 Soil Survey Staff. 2014. Keys to Soil Taxonomy, 12th ed. USDA-Natural Resources Conservation Service,

549 Washington, DC.

550 Stoops G., 2003. Guidelines for Analysis and Description of Soil Regolith Thin-Sections. Soil Science Society of

551 America, Madison.

552 Takeda, H. 1988. A rapid method for preparing thin sections of soil organic layers. Geoderma 42, 159-164

553 Tippkötter, R., Ritz, K., Darbyshire, J.F., 1986. The preparation of soil thin sections fo biological studies. Eur.

554 J. Soil Sci. 37, 681-690.

555 Tisdall J.M., Oades J.M.. 1982. Organic matter and water-stable aggregates in soils. J. Soil Sci. 33:141–163.

556 Totsche, K.U., Martin, W.A., Gerzabek H., Guggenberger G., Klumpp E., Knief C., Lehndorff E., Mikutta R.,

557 Peth S., Prechtel A., Ray N., Kögel-Knabner, I., 2017, Microaggregates in soils. J. Soil Sci. Plant Nutr. 181, 104-

558 163.

559 Toosi, E. R., Kravchenko, A. N., Mao, J., Quigley, M. Y., and Rivers, M. L., 2017. Effects of management and

560 pore characteristics on organic matter composition of macroaggregates: evidence from characterization of

561 organic matter and imaging. Eur. J. Soil Sci. 68, 200-211.

562 Van Reeuwijk, L.P., 2002.Procedures for soil analysis. Technical Paper n. 9. International Soil Reference and

563 Information Centre, Wageningen, 11-1.

564   Vittori Antisari, L., Carbone, S., Gatti, A., Vianello, G., Nannipieri, P., 2014. Uptake and translocation of metals

565   and nutrients in tomato grown in soil polluted with metal oxide (CeO_2, Fe_3O_4, SnO_2, TiO_2) or metallic (Ag, Co,

566   Ni) engineered nanoparticles. Environ. Sci. Pollut. Res. 22, 1841-1853.

567   Wang, Y. Hu, N., Ge, T., Kuzyakov, Y., Wang, Z-L., Li, Z., Tang, Z., Chen, Y., Wu, C., Lou, Y. 2017. Soil aggregation

568   regulates distributions of carbon, microbial community and enzyme activities after 23-year manure

569   amendment. Appl. Soil Ecol. 111, 65-72

570   Wang, R., Dorodnikov, M., Yang, S., Zhang, S., Zhang, Y., Filley, T.R., Turco, R.F., Zhang, Y., Xu, Z., Li, H., Jiang,

571   Y. 2015. Responses of enzymatic activities within soil aggregates to 9-year nitrogen and water addition in a

572   semi-arid grassland. Soil Biol. Biochem. 81, 159-167.

573   Wiesmeier, M., Urbanski, L., Hobley, E., Lang, B., von Lutzow, M., Marin-Spiotta, E., van Wesemael, B., Rabot,

574   E., LieB, M., Gracia-Franco, N., Wollschager, U., Vogel, HJ., Kögel-Knabner, I., 2019. Soil organic carbon

575   storage as a key function of soil – A rewiew of drivers and indicatori at various scales. Geoderma 333, 149-

576   162.

577   Yang, C., Liu, N., Zhang, Y., 2019, Soil aggregates regulate the impact of soil bacterial and fungal communities

578   on soil respiration. Geoderma 337, 444-452.

579   Young I.M., Crawford J.W., Nunan N., Otten W., Spiers A., 2008. Microbial distribution in soils: physics and

580   scaling, in: Sparks, D.L. (Ed.). Advances in Agronomy. Academic Press, Burlington, pp. 81–121.

581   Zhou, H., Peng, X., Pech, S., Xiao, T.Q., 2012. Effects of vegetation restoration on soil aggregates

582   microstructure quantified with synchrotron-based micro-computed tomography. Soil Till. Res. 124, 17-23.

583

584

585   **Figure captions**

586   Figure 1. Pore size distribution in a) coarse and b) fine macroaggregates. In c) the ANOVA results are

587   reported. M-OW and M-AA: 16-yrs old oak wood and 5-yrs old alfalfa in mountain area, respectively; P-NF

588   and P-FF: non-fertilized and fertilized walnut grove in plain area.

589   Figure 2. Al:C, Fe:C and Ca:C molar ratio of the different organic forms in coarse and fine macroaggregates.

590   Different capital letters represent the significant diffences among organic forms. Different lower letters

591   represent the significant difference between coarse and fine macroaggregates within the same organic

592   forms.

593   Figure 3. Box-plots of exposure index (EI, in mm^{-1}) values in the coarse and fine macroaggregates. The box

594   represents the interquartile range, the line represents the median value, the symbol represents the mean

595   value, error bars represent the full range of data. Different letters refer to significant differences ($p < 0.05$)

596   Figure 4. Relationships between EI values measured in aggregate thin sections and chemical properties

597   measured on ground aggregates (C/N ratio and δ^{13}C). The coarse (filled symbols) and fine macroaggregate

598   (open symbols) classes are display for each plot. The error bars indicate the standard deviation.

599   Figure 5. Relationships between EI values measured in aggregate thin sections and geometric mean of

600   assayed enzyme activities (GM*ea*). The coarse (filled symbols) and fine macroaggregate (open symbols)

601   classes are display for each plot. The error bars indicate the standard deviation.

602   Figure 6. Conceptual scheme of macroaggregates and organic matter stabilization. Into brackets the

603   microfeatures used in this study and suggesting each step of the scheme
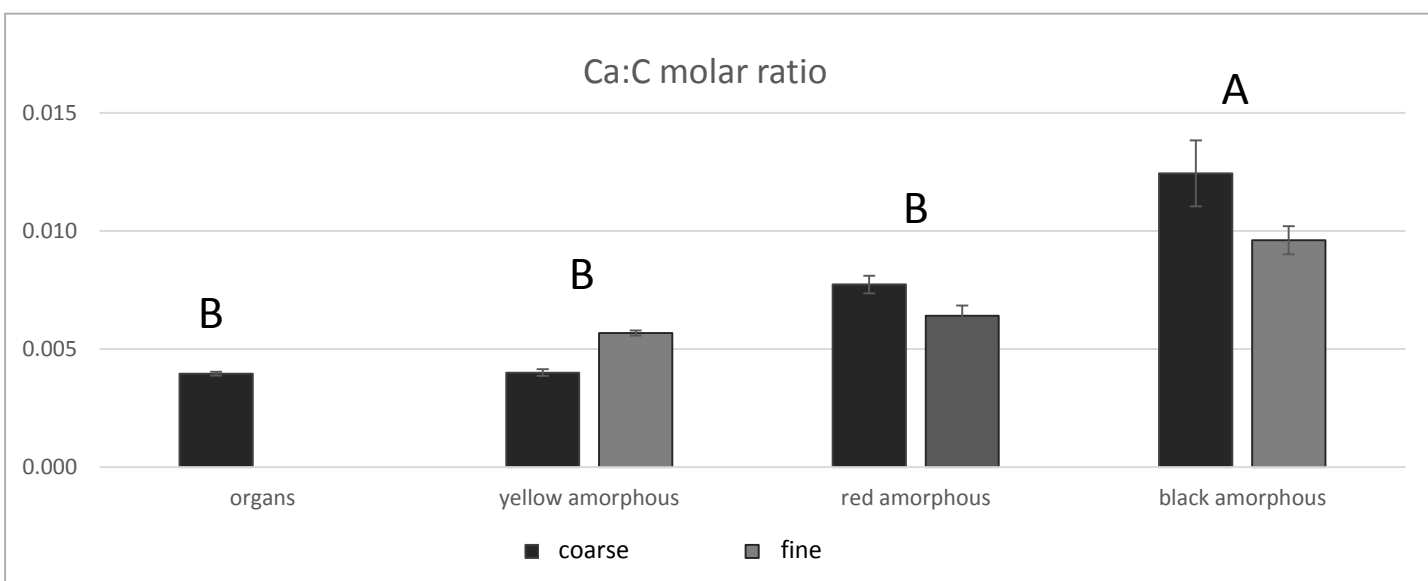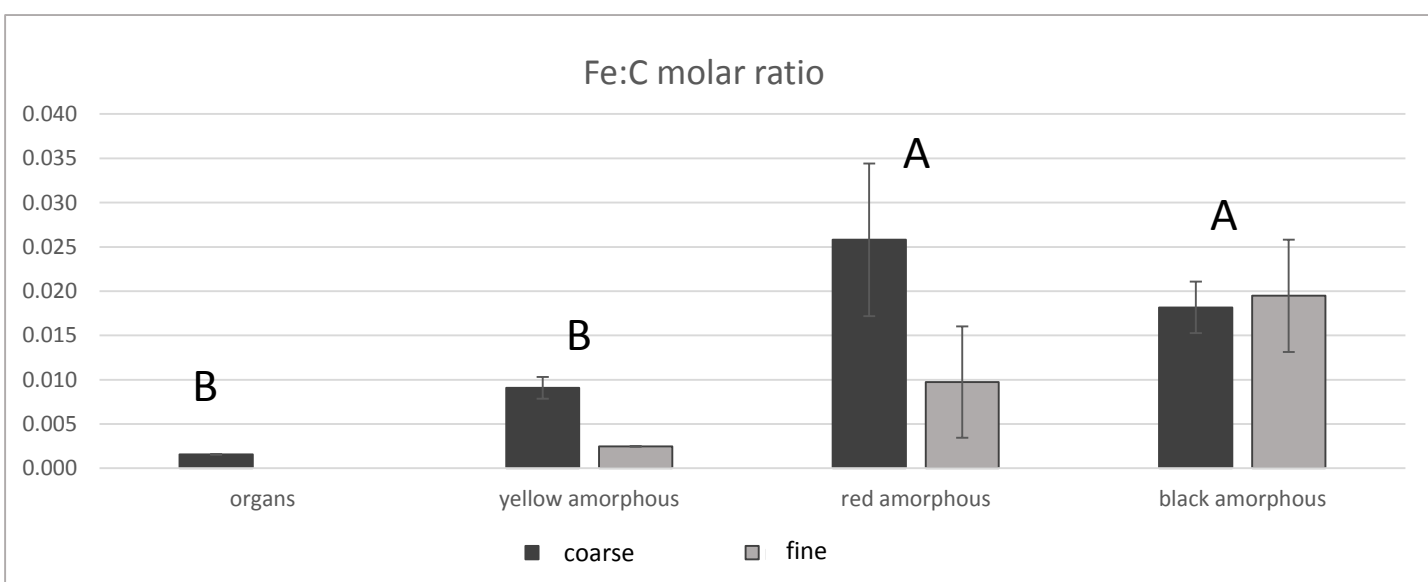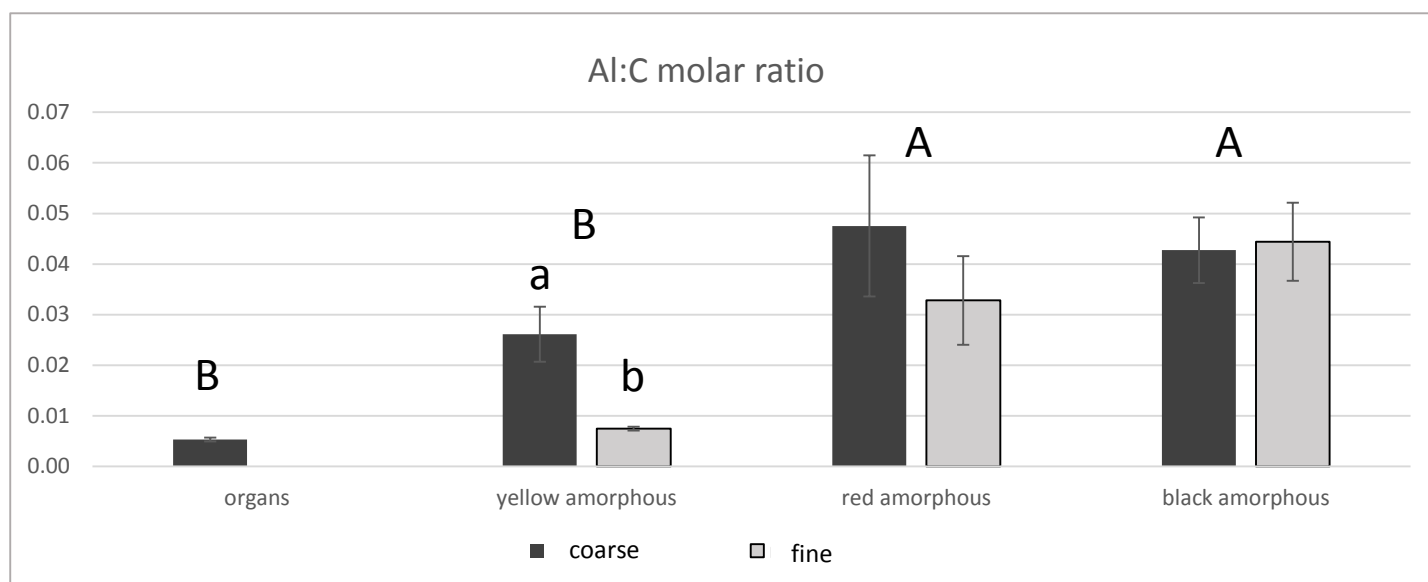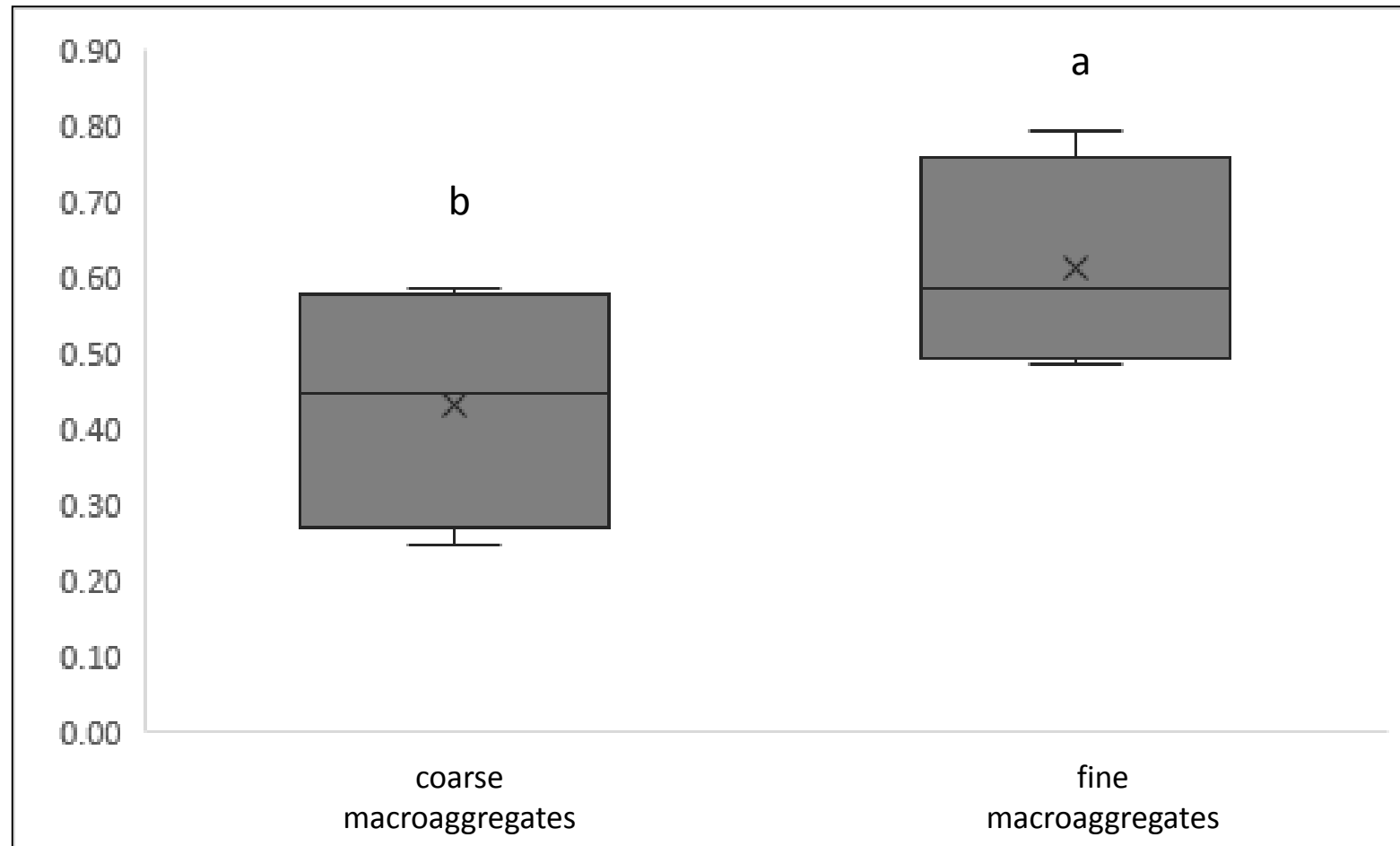
604

a), b) Stacked bar charts showing particle size distribution (<50 μm, 50-100 μm, 100-200 μm, >200 μm) for M-OW, M-AA, P-NF, P-FF.
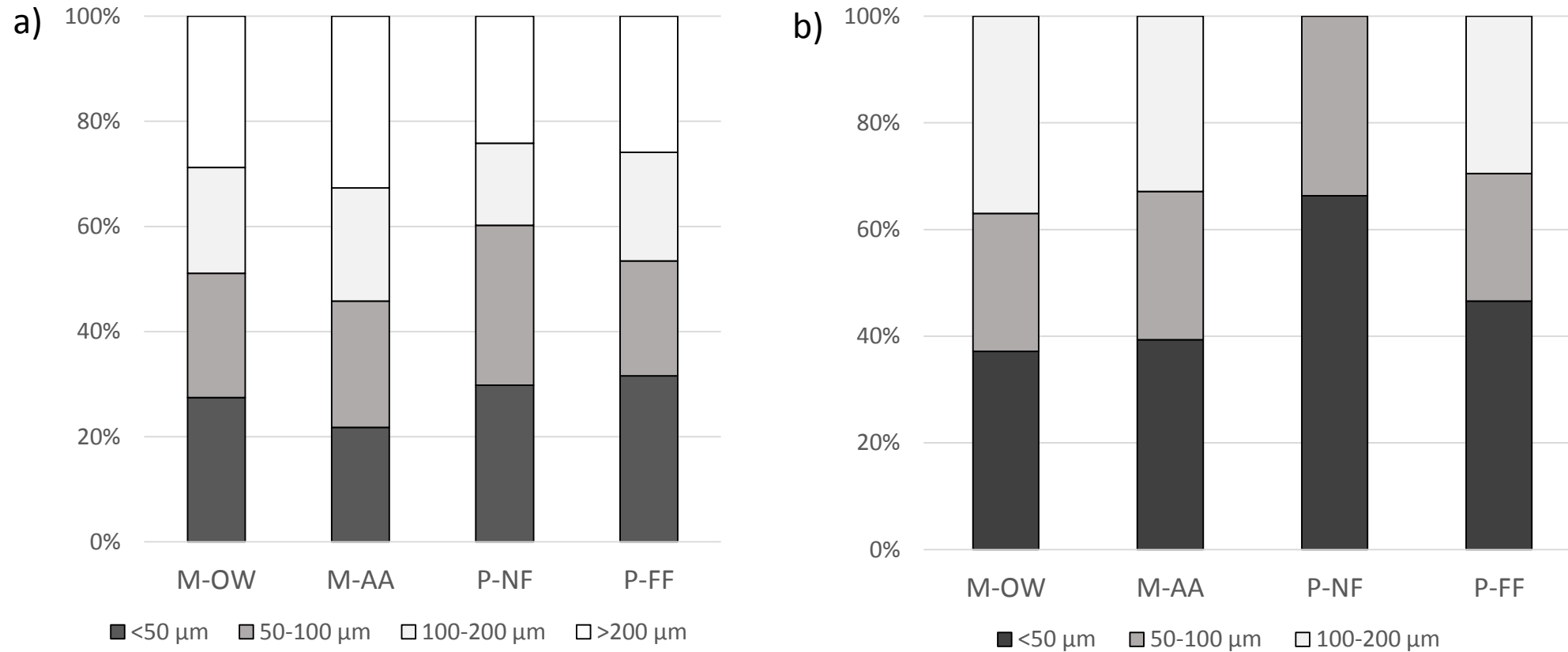
c)

		<50 μm (%)	50-100 μm (%)	100-200 μm (%)	>200 μm (%)
coarse *vs* fine macroaggregates		***	**	***	nd
within coarse macroaggregates	site	ns	ns	ns	ns
within fine macroaggregates	site	ns	ns	ns	nd

ns: not significant (p>0.05);*: p<0.05; **: p<0.01; ***: p<0.001

nd: not determined

Figure 2

Figure 3

Figure 4

Figure 5 Click here to access/download;Figure;Figure 5.pptx ⬇

Figure 5

Figure 6
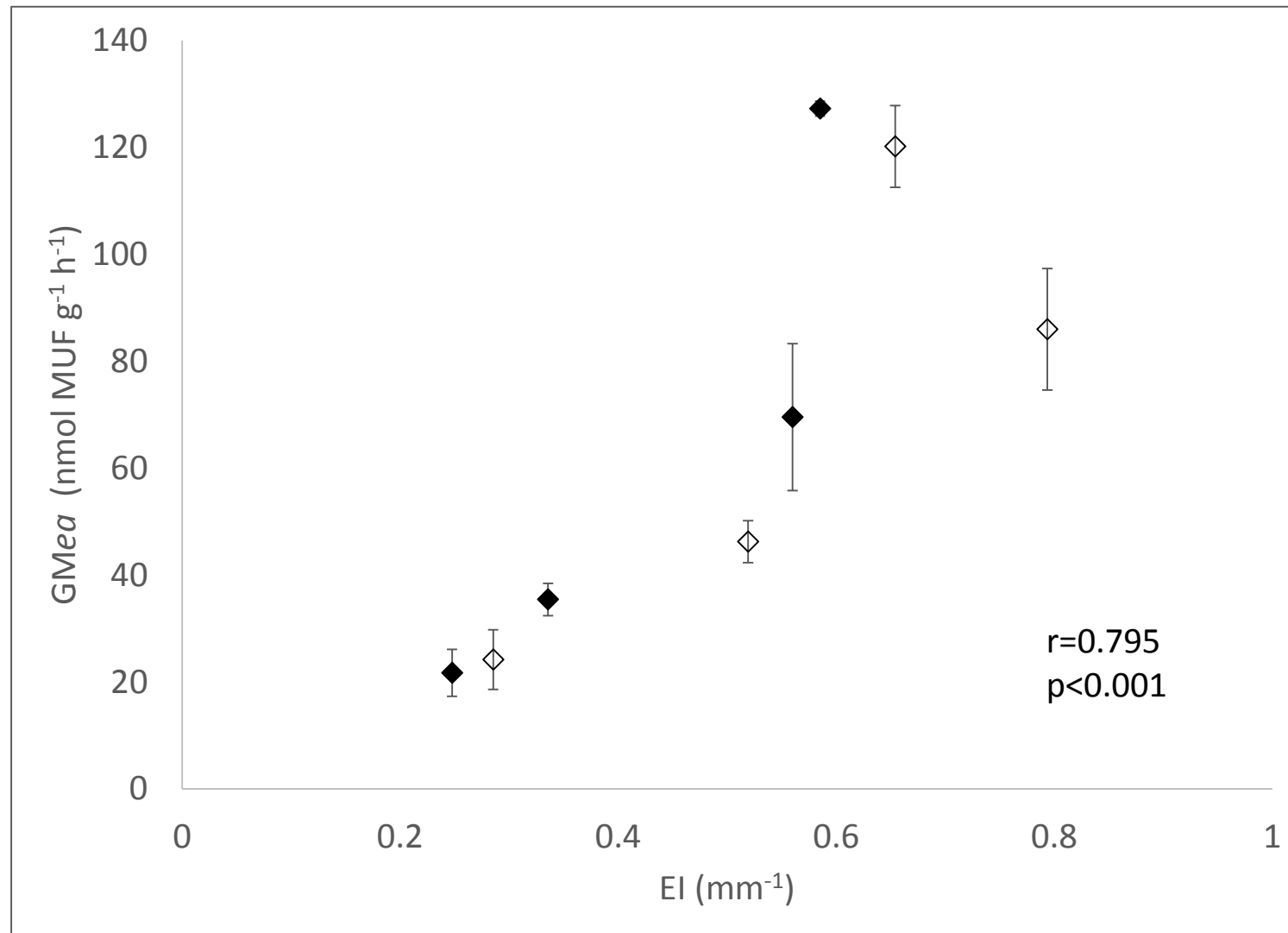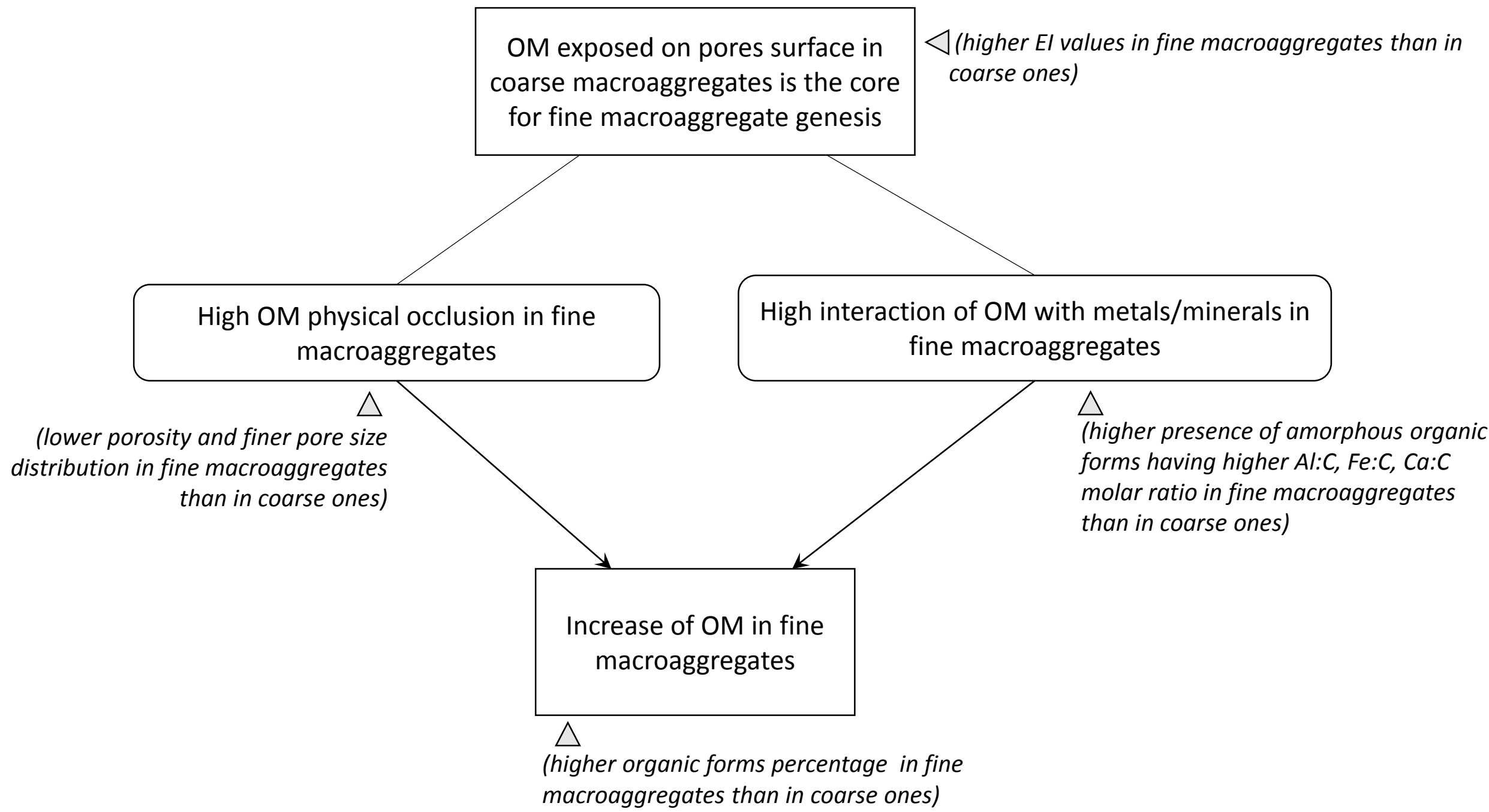
Figure 6
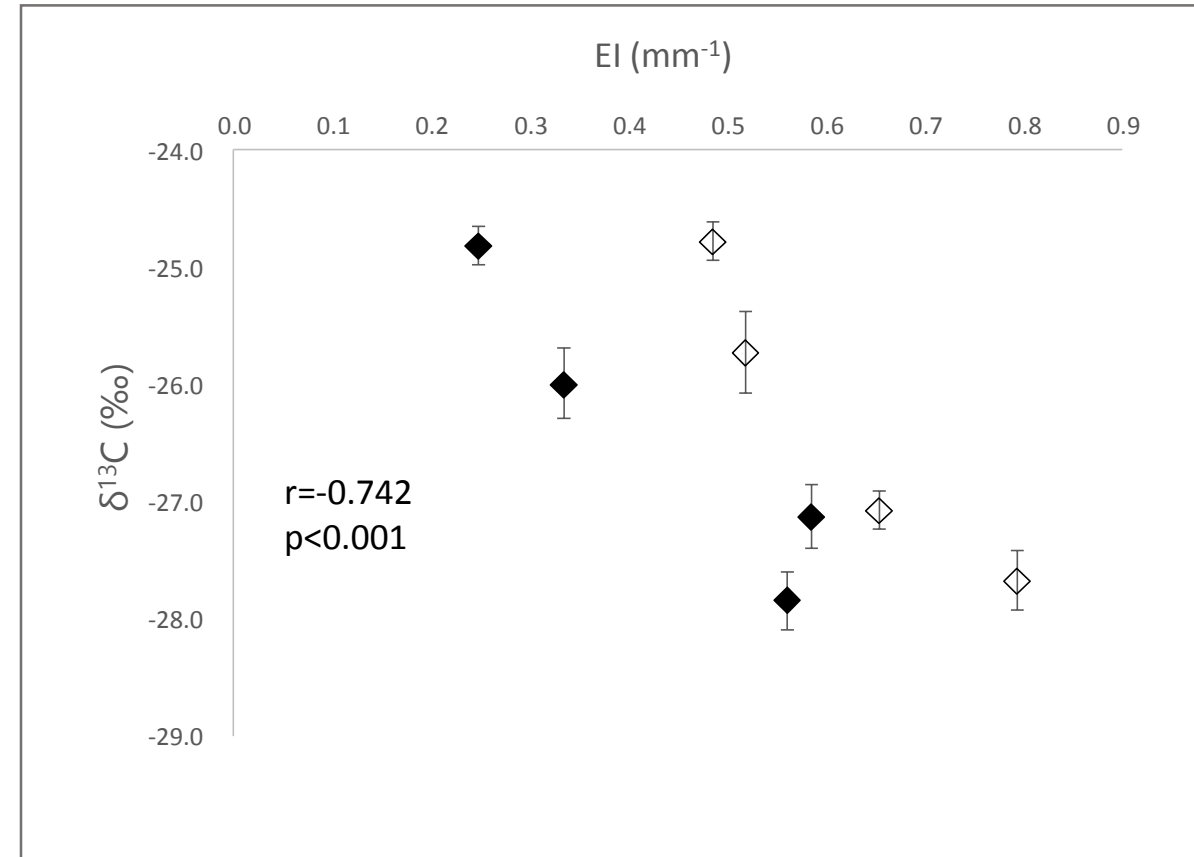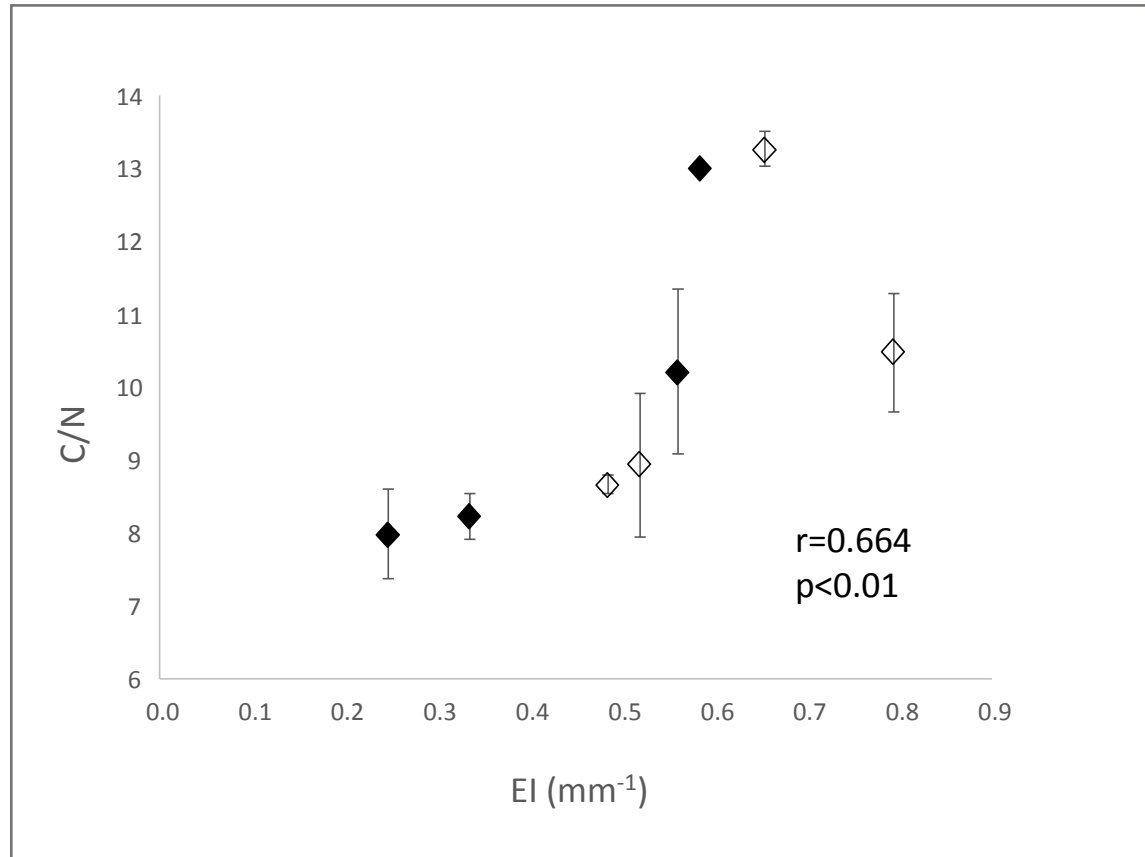
Table 1. General information of the investigated sites

Area (climate/soil type)	Site	Coordinates	Elevation (m a.s.l.)	Soil management and sampling information
Mountain (MAT: 11.6°C; MAP: 967 mm/Inceptisols)	M-OW	44° 16'29''N 11°14'53''E	630	The oak wood was a 16-year-old wood exploited for firewood. At sampling time, the wood was at the end of its cutting cycle.
	M-AA	44°16'28''N 11°15'25''E	663	The alfalfa was a 5-year-old crop not-fertilizer. At sampling time, the alfalfa was at the end of its cropping cycle.
Plain (MAT: 12.9°C ; MAP: 645 mm/Inceptisols)	P-FF	44°32'18''N 11°23'07''E	34	Since 2001, 90 kg/ha/yr g of urea has been distributed for granular treatment subdividing in two doses (45 kg/ha/yr g in April/May and 45 kg/ha/yr in October). The soil was not tilled and covered by spontaneous grasses. The soil sampling was done along the plant rows.
	P-NF	44°32'19''N 11°23'07''E	34	Since 2001, the site was not fertilized. The soil was not tilled and covered by spontaneous grasses. The soil sampling was done along the plant rows.

MAT: mean annual temperature; MAP: mean annual precipitation

Table 2. Percentage of total porosity, organic carbon and presence of organic matter forms in coarse and fine macroaggregates. Numbers in the brackets represent the standard deviation values. In the bottom, the ANOVA results are reported

Macroaggregate class	Sites	Total porosity[a] (%)	Organic carbon[b] g kg^{-1}$_{aggregate}$	Organic matter forms[a] (%)
coarse	M-OW	5.96 (1.67)	49.6 (4.6)	8.27 (1.29)
	M-AA	9.08 (1.00)	10.9 (3.5)	6.51 (0.95)
	P-NF	5.93 (1.89)	6.6 (1.8)	4.19 (0.88)
	P-FF	8.19 (1.43)	7.9 (1.2)	5.58 (1.10)
fine	M-OW	4.42 (0.97)	52.4 (7.3)	17.2 (4.48)
	M-AA	6.71 (1.43)	12.1 (3.4)	17.7 (1.94)
	P-NF	3.70 (0.78)	7.8 (1.2)	14.4 (2.99)
	P-FF	6.53 (1.18)	9.3 (3.0)	13.5 (3.41)
coarse *vs* fine macroaggregates		***	ns	***
within coarse macroaggregates	site	ns	***	ns
within fine macroaggregates	site	ns	**	ns

[a]measured on macroaggregate thin sections; [b]measured on grounded macroaggregates.

M-OW and M-AA: 16-yrs old oak wood and 5-yrs old alfalfa in mountain area, respectively; P-NF and P-FF: non-fertilized and fertilized walnut grove in plain area.

ns: not significant ($p > 0.05$); **:$p < 0.01$; ***: $p < 0.001$

Table 3. Organic matter forms distribution in coarse and fine macroaggregates. Numbers in the brackets represent the standard deviation values

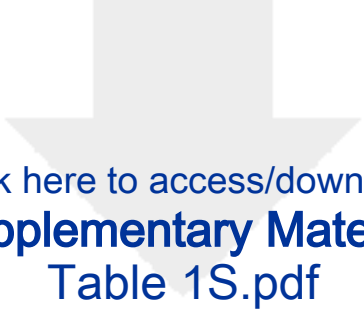| macroaggregate class	sites	Organs (%)	Yellow amorphous forms (%)	Red amorphous forms (%)	Black amorphous forms (%)
coarse	M-OW	3.31 (0.9)	1.87 (0.2)	2.32 (0.6)	3.16 (0.7)
	M-AA	1.11 (0.4)	-	2.09 (0.9)	3.51 (0.3)
	P-NF	-	1.10 (0.4)	1.29 (0.3)	2.07 (0.4)
	P-FF	-	1.10 (0.5)	2.14 (0.5)	3.14 (0.7)
fine	M-OW	-	1.21 (0.4)	7.77 (0.8)	8.51 (1.2)
	M-AA	-	1.84 (0.8)	6.07 (0.7)	12.1 (1.2)
	P-NF	-	-	6.64 (0.7)	9.72 (1.5)
	P-FF	-	-	5.65 (0.8)	5.30 (0.9)
coarse *vs* fine macroaggregates		-	-	***	***
within coarse macroaggregates	site	-	-	*	*
within fine macroaggregates	site	-	-	***	***

M-OW and M-AA: 16-yrs old oak wood and 5-yrs old alfalfa in mountain area, respectively; P-NF and P-FF: non-fertilized and fertilized walnut grove in plain area.

ns: not significant (p>0.05); *:p<0.05; ***: p<0.001

Declaration of interests

☒ The authors declare that they have no known competing financial interests or personal relationships that could have appeared to influence the work reported in this paper.

☐ The authors declare the following financial interests/personal relationships which may be considered as potential competing interests:

Click here to access/download
Supplementary Material
Table 1S.pdf

Click here to access/download
Supplementary Material
Supplementary material_rev.pptx